Original article

Efficacy and Safety of a novel virulent phage against acute pulmonary infection of *Acinetobacter baumanniii* in mice

JiaWang.Wang[123], Huan.Hu[23], QingQing.Wang[23],TianZhu.Zhu[23],XiaoHan.Ren[23],WenQian.Jiang[23], XueMei.Hou[*23],Jun.Lin[*23],XiaoLing.Yu[*123]

1) Department of Pharmacy, Mengchao Hepatobiliary Hospital of Fujian Medical University, Fuzhou 350025, China;
2) Institute of Applied Genomics, Fuzhou University, Fuzhou 350108, China;
3) College of Biological Science and Engineering, Fuzhou University, Fuzhou 350108, China;
* Corresponding author
Xiaoling.Yu: Department of Pharmacy, Mengchao Hepatobiliary Hospital of Fujian Medical University, Fuzhou, China; 350025;E-mail:xiaolingyu82@163.com;Tel: +86 591 88116019;
Jun.Lin: Institute of Applied Genomics, College of Biological Science and Engineering,Fuzhou University, Fuzhou, China;350108; E-mail: jun@fzu.edu.cn;Tel: +86 591 22863805;
XueMei.Hou: Institute of Applied Genomics, College of Biological Science and Engineering,Fuzhou University, Fuzhou, China;350108; E-mail: houxuemei_1990@163.com;Tel: +86 591 22863805;

Abstract

Background: *Acinetobacter baumanniii* (*A.baumannii*) is an opportunistic pathogen that significantly contributes to the burden of hospital-acquired infections. The treatment of multidrug-resistant *A.baumannii* poses a major challenge due to its resistance to multiple antibiotics.Phage therapy, leveraging bacteriophages as natural bacterial predators, has re-emerged as a promising approach to combat antibiotic-resistant infections.
Objectives: This study aimed to isolate and characterize phages targeting *A.baumannii* from environmental samples, establish a comprehensive phage characterization process, and evaluate the therapeutic efficacy and safety of this phage using a mouse model with pneumonia.
Methods: The following are the methods used for this study.
Results: This study identified vB_AbaS_qsb1, a novel virulent phage which had never been reported that specifically lyses *A.baumannii*. The vB_AbaS_qsb1 exhibits robust stability across a broad temperature and pH range, a short incubation period. Genomic analysis showed that qsb1 has a 54,713 bp dsDNA genome with a GC content of 39%, lacking any known virulent factor or antibiotic resistance genes. Importantly, safety evaluations demonstrated that high-dose vB_AbaS_qsb1 did not induce any adverse clinical symptoms in mice, further underscoring the phage's excellent safety profile as confirmed by other experimental results.Therapeutic experiments showed that vB_AbaS_qsb1 provided at least 50% protection against acute pneumonia causing by *A.baumannii*, with a significant reduction in lungs' bacterial loads and sustained high

phage titers. Inflammatory markers in phage-treated mice were significantly lower than those in untreated groups, underscoring the phage's effective bacterial clearance and reduction of inflammation.

Conclusions: This study highlights the therapeutic potential of a novel phage vB_AbaS_qsb1 against *A.baumannii*, especially amid rising antibiotic resistance. With its safety confirmed, vB_AbaS_qsb1 showed potent antibacterial activity both in vitro and in vivo, significantly reducing bacterial loads and improving survival in mouse models. This research also provides a valuable framework for the isolation, genomic analysis, and evaluation of *A.baumannii* phages.

Graphical abstract

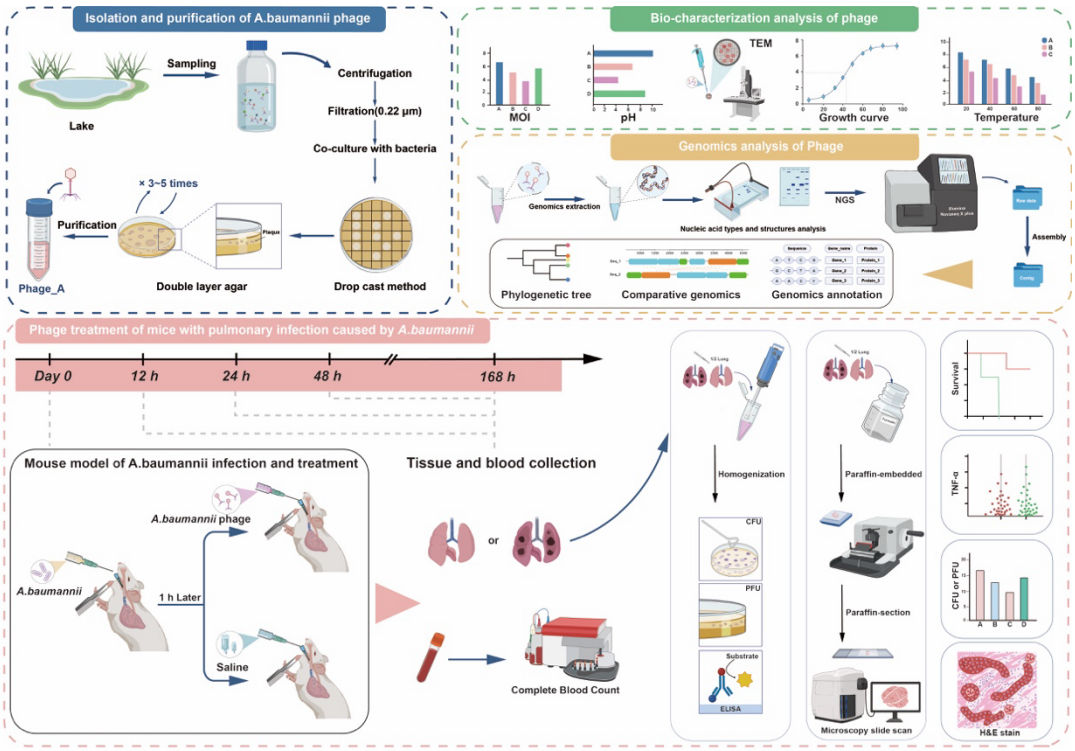

Introduction

A.baumannii is a Gram-negative, non-motile opportunistic pathogen commonly found in aquatic and soil environments, and a leading cause of nosocomial infections. It is associated with high mortality rates, particularly in ICU settings where infections such as pneumonia and sepsis can result in mortality rates as high as 54%[1, 2]. This pathogen is a major contributor to lung infections, sepsis, meningitis, urinary tract infections, and wound infections[3].

In clinical practice, antibiotics are commonly used to treat *A.baumannii* infections, but the misuse of these drugs has led to the rise of multidrug-resistant (MDR) strains, including carbapenem-resistant *A.baumannii* [4]. While combination antibiotic therapy is employed to combat resistance[5], its effectiveness can be limited by antagonistic interactions and may even promote broad-spectrum resistance[6]. The high mortality rate of *A.baumannii* infections stems from its inherent resistance and ability to acquire resistance genes[7, 8]. In response, the WHO classified carbapenem-resistant *A.baumannii* as a critical priority for antibiotic development in 2017, reaffirming its importance in 2024[9, 10].

Given the escalating challenge of antibiotic resistance, the need for novel antimicrobial treatments is pressing. Phage therapy, an ancient yet increasingly promising approach, has garnered renewed interest. Bacteriophages are viruses that specifically infect bacteria, and based on their lifecycle, they can be categorized as either virulent or temperate[11]. Due to their ability to specifically lyse bacterial pathogens without harming eukaryotic cells, virulent phages have emerged as potential therapeutic agents for treating bacterial infections[12]. In vitro studies have demonstrated the potent antibacterial activity of phages, showing their ability to effectively eliminate bacteria and disrupt biofilms[13, 14]. Furthermore, in vivo studies of animals have confirmed the safety and efficacy of phage therapy in treating bacterial infections[15, 16]. Numerous compassionate-use cases have highlighted the clinical success of phage therapy in treating various infections, including lung infections[17, 18], pancreatic infections[19], osteomyelitis[20], and enteritis[21].

In this study, we isolated and systematically characterized a novel virulent phage targeting *A.baumannii* from environmental sewage, detailing its biological properties and genomic features. This phage has been preserved in the Guangdong Microbial Culture Collection Center(GDMCC), with the accession number GMDCC 64831-B1. Additionally, we established a mouse model of *A.baumannii*-induced pneumonia to assess the phage's safety and antibacterial efficacy in vivo. This model is essential for evaluating the phage's therapeutic potential in reducing bacterial load, improving survival rates, and ensuring safety, providing a foundation for future clinical applications.

Result

Purification and morphology of a novo-bacteriophage vB_AbaS_qsb1

A potent *A.baumannii* phage, vB_AbaS_qsb1, was successfully isolated from local lake(QiShan lake, FuZhou city, FuJian provience, China) water sample, utilizing *A.baumannii* strain *ioag01* as the host. Following preprepared double-layer agar plates seeded with qsb1 and *ioag01*, and subsequent incubation at 37℃ overnight, distinct plaques with an average diameter of approximately 4.0±1.0 mm were observed, accompanied by a depolymerase halos with an approximate measurement of 7.0±1.0 mm (Figure 1A).Transmission electron microscopy (TEM) analysis (Figure 1B) revealed that the phage's head dimensiona were approximately 70×80 nm, with a tail extending about 90 nm in length and a tail diameter of 20 nm. In accordance with the International Committee on Taxonomy of Viruses (ICTV) classification and nomenclature criteria, the phage was designated as vB_AbaS_qsb1. The phage has been archived in the Guangdong Microbial Culture Collection Center (GDMCC) with the accession number GMDCC 64831-B1.

The study of the biological characteristics of qsb1 showed that the optimal phage replication efficiency was achieved at an multiplicity of infection (MOI) of 0.1 (Figure 1C). At this MOI, phage proliferation exhibited a two-log increase within 6 hours under these conditions. The one-step growth curve of qsb1 revealed a short latent period (about 20 minutes), followed by an exponential phase(about 100 minutes), with a burst size of approximately 23 plaque-forming units (PFU) /cell (Figure 1D).Thermal stability analysis demonstrated that qsb1 remains stable between 10 ℃ and 60 ℃, though the phage lost all activity at 80 ℃ and 100 ℃ (Figure 1E). pH stability testing indicated qsb1 stability across a pH range of 3 to 11, with significant reductions in activity observed at pH 1 and complete inactivation at pH 13 (Figure 1F). Overall, qsb1 shows robust stability under normal physiological conditions, with activity only compromised under extreme heat or pH levels.

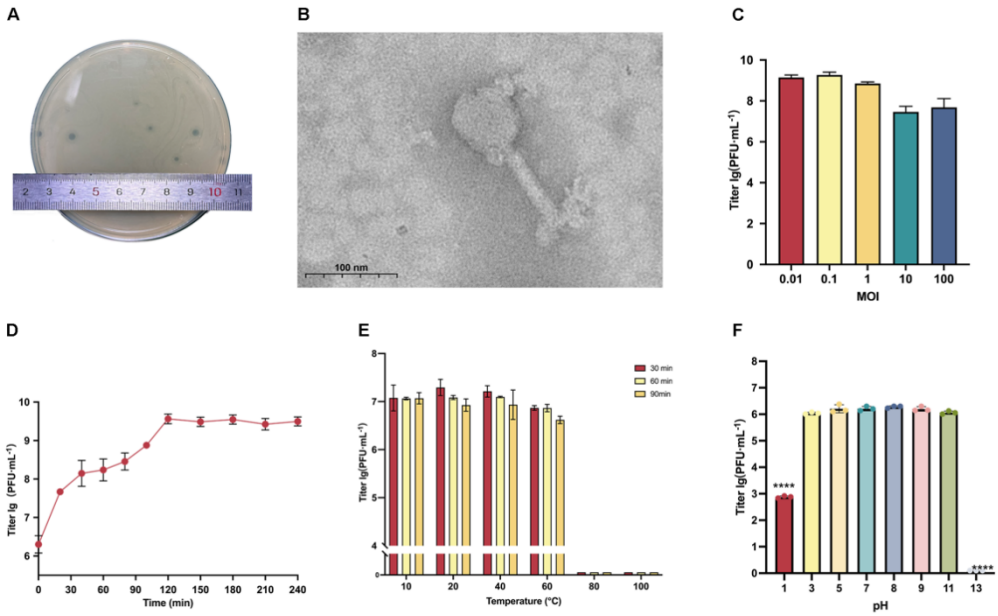

Figure 1: Biological Characteristics of Bacteriophage vB_AbaS_qsb1

(A) Plaque morphology of vB_AbaS_qsb1 on double-layer agar plates. When vB_AbaS_qsb1 and *ioag01* were co-cultured in soft agar overnight at 37℃, clear transparent plaques and distinct

depolymerase halos were observed.

(B) Transmission electron microscopy (TEM) image of vB_AbaS_qsb1 morphology, negatively stained with 4% phosphotungstic acid, The scale bar corresponds to 100 nm.

(C) MOI of vB_AbaS_qsb1, showing phage titer following infection of its host at various MOIs.

(D) One-step growth curve of vB_AbaS_qsb1.

(E) Temperature stability of vB_AbaS_qsb1, represented by titer variations at different temperatures across varying time periods.

(F) pH stability of vB_AbaS_qsb1. All samples were analyzed in triplicate, and the results are expressed as mean values ±SD.

Genome characteristics of the phage vB_AbaS_qsb1

Genome features of phage vB_AbaS_qsb1

Pulsed-field gel electrophoresis (PFGE) estimated the genome size of vB_AbaS_qsb1 to be approximately 50 kbp (Supplementary Figure S1). Next-generation sequencing (NGS) revealed that the qsb1 genome comprises 54,713 base pairs(Figure 2A) of double-stranded DNA (verified using RNase A and S1 nuclease; Supplementary Figure S2), with a GC content of 39%. A total of 95 coding DNA sequences (CDSs) were identified, numbered from CDS_1 to CDS_95 (Supplementary Table S1). Among these, 42 CDSs were predicted to encode proteins with known functions, while the remaining 51 were classified as hypothetical proteins with uncharacterized roles. The identified proteins are involved in key biological processes such as structural assembly, DNA replication and repair, gene regulation, host recognition, and infection mechanisms. Notably, an integrase gene (CDS_1), typically associated with lysogeny, was identified, but experimental data and lifestyle prediction analyses confirmed that qsb1 functions as a virulent phage in both in vivo and in vitro studies. Additionally, the genome encodes a depolymerase (CDS_12), likely enhancing the phage's ability to degrade extracellular polysaccharides, aiding in bacterial lysis and biofilm disruption. Comprehensive scans using CRAD and Phagescope did not detect any virulence or antibiotic resistance genes, indicating that qsb1 is a promising and safe candidate for phage therapy.

Phylogenetic analysis

The complete genomic sequence of vB_AbaS_qsb1 was submitted to NCBI for BLASTn analysis. By comparison, the top 15 phages with the highest sequence similarity were chosen to construct a phylogenetic tree. The analysis indicated that vB_AbaS_qsb1 is most closely related to *A.baumannii phage BUCTT20*, as evidenced by their co-location within the same phylogenetic branch (Figure 2B). Additionally, a whole-genome synteny comparison between vB_AbaS_TRS1 and qsb1 was conducted based on NCBI data, revealing that qsb1 had reduced genome coverage compared to other analyzed phages, with 7% and 20% coverage against BUCTT20 and vB_AbaS_TRS1(Figure 2C).In summary, we identified and characterized a novel bacteriophage, vB_AbaS_qsb1, which represents a new species with potent lytic activity against *A.baumannii*. Its unique genomic features and strong antibacterial efficacy distinguish it from previously known phages, highlighting its potential as a promising therapeutic agent against multidrug-resistant A. baumannii infections.

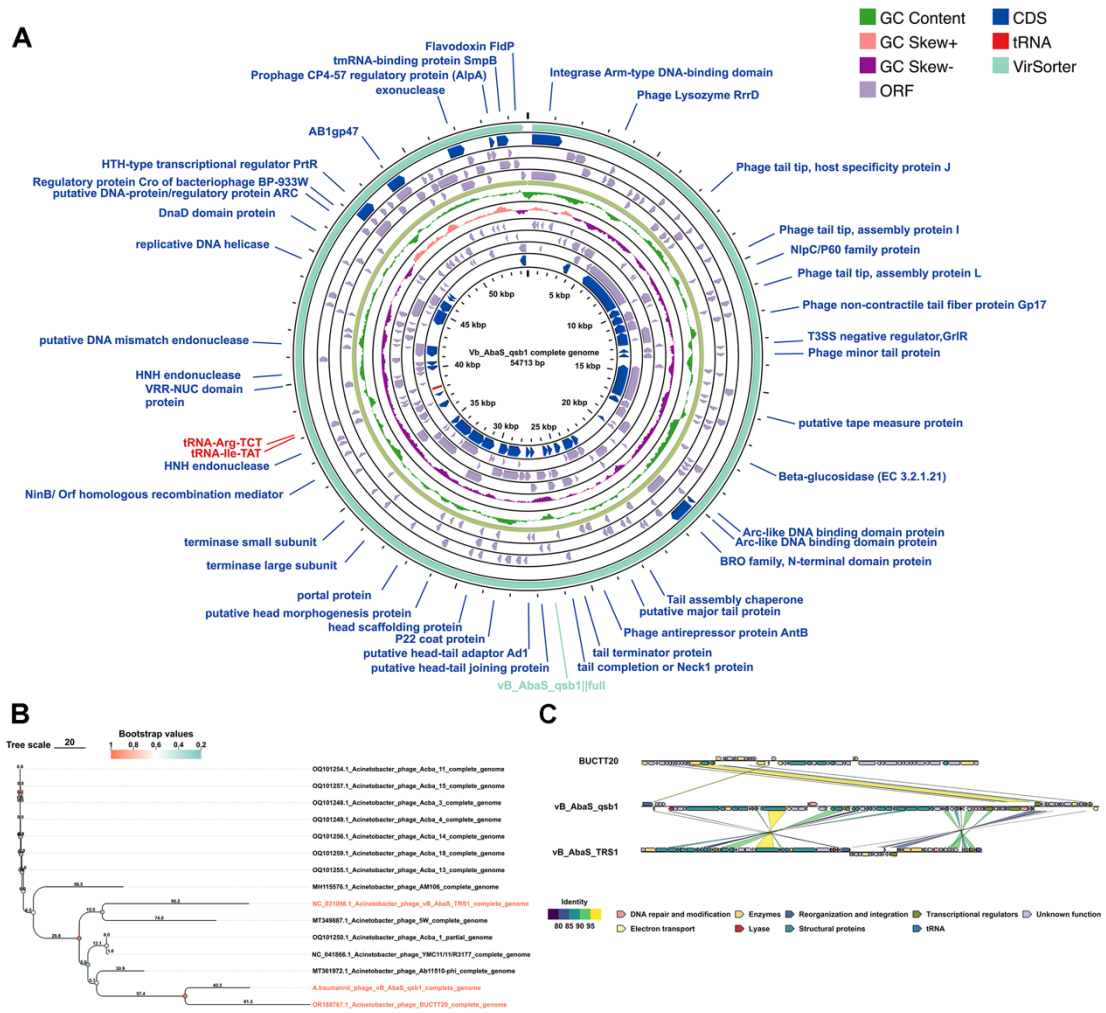

Figure 2: Whole-Genome Circular Map, Phylogenetic Tree, and Collinearity Analysis of Bacteriophage vB_AbaS_qsb1.

(A) Circular map of the vB_AbaS_qsb1 genome. The green ring represents the GC content, while the pink and dark purple rings display the CG skew for the positive and negative strands, respectively. Lavender rings denote predicted open reading frames (ORFs), and dark blue rings correspond to coding sequences (CDSs) annotated with predicted protein functions. Red labels indicate tRNAs, and mint green highlights identifiable viral sequences. Pseudogenes or proteins of unknown function are excluded from the map.

(B) Phylogenetic tree of vB_AbaS_qsb1, constructed based on whole-genome sequence analysis. Bootstrap values (range: 0 to 1) are indicated by circles at branch nodes to assess the reliability of the tree topology. The scale bar represents the degree of sequence divergence between phages.

(C) Collinearity comparison of the vB_AbaS_qsb1 genome with vB_AbaS_TRS1 and BUCTT20. Arrows indicate the location and orientation of CDSs in each genome (right-pointing arrows for the positive strand, left-pointing arrows for the negative strand). The lines between genomes illustrate sequence similarities (as represented in the bottom left corner), and CDSs are color-coded by functional categories, as shown in the legend in the bottom right corner.

Phage therapy for acute pulmonary infection caused by *A.baumannii* in mice

Establishment of the model of pulmonary infection caused by *A.baumannii* in mice

A BALB/C mouse model of acute pulmonary infection caused by *A.baumannii* was established by tracheal instillation of bacteria directly into the trachea.

Over the course of a 7-day observation period, all mice in the 3×10^9 Colony-forming units (CFU)/mouse group died within 36 hours, and those in the 3×10^8 CFU/mouse group had a mortality rate of 83.3%. In contrast, only one mouse in the 3×10^7 CFU/mouse group succumbed (a mortality rate of 16.7%), and no mortality was observed in either the 3×10^6 CFU/mouse group or the control group (Figure 3A). Based on the median lethal dose (LD_{50}) criteria and to ensure the study's comparability, a bacterial dose of 3×10^8 CFU/mouse was selected for subsequent experiments to construct a reliable model of pulmonary infection in mice.

The Safety of phage therapy

To assess whether *A.baumannii* phage qsb1 induces severe immune responses or adverse clinical symptoms in mice, phage preparation was instilled into the lungs. Throughout the 7-day observation period, none of the mice in the phage-treated group exhibited any negative clinical symptoms, and no deaths occurred (Figure 3A). Whole blood samples of mice were collected for complete blood count（CBC）. The results indicated no significant differences in the levels of white blood cells and neutrophils between the phage-treated group and the control group (Figure 3B). Furthermore, hematoxylin-eosin (HE) staining analysis (Figure 3C) revealed no significant infiltration of inflammatory cells in the lung tissue, no apparent congestion, and the alveolar structure remained intact. Summary, no severe immune responses or lung tissue damage were observed in mice treated with phage qsb1, confirming its safety.

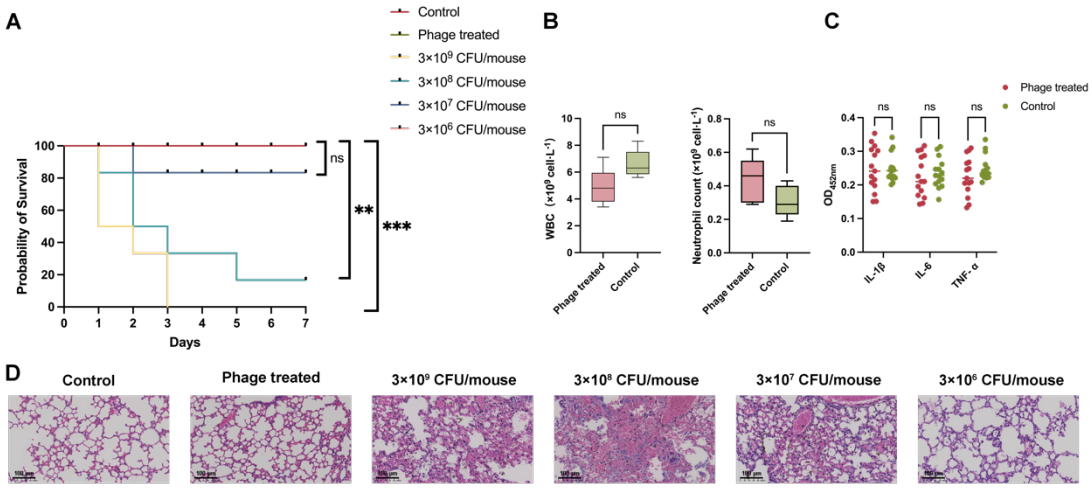

Figure 3: Mouse model of *A.baumannii* lung infection and phage safety evaluation. The control group received saline treatment only, while the phage-treated group received 10^9 PFU of qsb1. Other groups were administered varying doses of *A.baumannii* culture.

(A) Survival curve of mice during the 7-day observation period (n=6 for the Control, 3×10^9 CFU/mouse, 3×10^8 CFU/mouse, 3×10^7 CFU/mouse and 3×10^6 CFU/mouse, n=5 for the Phage treated group).

(B) Leukocyte and neutrophil counts in whole blood of the control and phage treated groups (n=5). The results indicate no significant differences in leukocyte and neutrophil levels between the phage-

treated and control groups.

(C) Relative levels of inflammatory cytokines (IL-1β, IL-6, and TNF-α) in mouse lung tissues (n=5). The data demonstrate no significant differences in the levels of IL-1β, IL-6, and TNF-α between the phage-treated and control groups.

Pathological examination of mouse lung tissue. Scale bar=100μm. Statistical analysis of survival curves was performed using the log-rank test, while other data were analyzed using two-way ANOVA. ***$p < 0.001$, **$p < 0.01$, *$p < 0.05$.

Phage treatment of mice with pulmonary infection caused by *A.baumannii*

To investigate the efficacy of different phage doses on the treatment of pneumonia-infected mice, phage therapy was administered 1 hour post-infection. In the Mock-treated group, a substantial number of mice (4/5) succumbed within 48 hours, resulting in a final survival rate of 20%. Similarly, in both the Medium-dose and Low-dose phage treated groups, most mice died (4/5) within 96 hours, with a survival rate of 20% by day 7. The survival rates in these groups were significantly lower than those observed in the control group. Remarkably, in the High-dose phage treated group, only one mouse died(1/5) following phage treatment, and the survival rate reached 80%, which was not significantly different from that of the control group (Figure 4A).

After the 7-day observation period, the mice were sacrificed, and blood samples were collected for CBC. The results showed no significant differences in leukocyte and neutrophil counts between the high-dose phage-treated group and the control group (Figure 4B). Histopathological examination of lung tissues with hematoxylin-eosin (HE) staining revealed substantial damage to the alveolar structure in the Mock, Medium-dose, and Low-dose treated groups, including a marked reduction in normal alveoli, inflammatory exudates in the alveolar spaces, thickened and ruptured alveolar septa, and significant congestion and necrosis of lung tissue. In contrast, the high-dose treated group displayed well-preserved lung architecture, with intact alveoli and no evident pathological changes, closely resembling the control group's lung morphology (Figure 4C). In summary, high-dose phage therapy significantly enhances the survival rate of infected mice and effectively prevents the development of lung lesions.

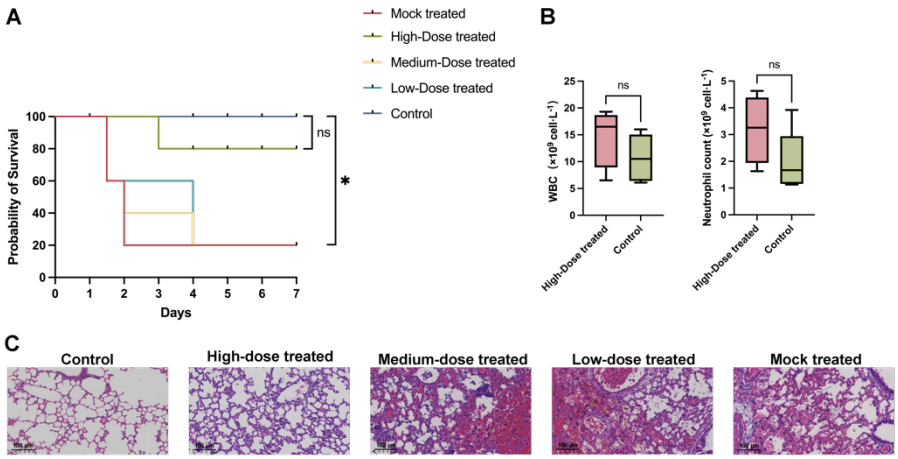

Figure 4: Phage therapy in lung-infected mice via tracheal instillation. The control group received only saline without infection, while the Mock-treated group was administered 3×10^8 CFU of *A.baumannii ioag01* without any treatment. Mice in the high, medium, and low-dose phage

treatment groups were administered 3×10^9, 3×10^8, and 3×10^7 PFU of qsb1, respectively, following infection.

(A) Survival curve of mice over 7 days following treatment with different doses of phage (n=5).

(B) White blood cell and neutrophil counts in mice 7 days post high-dose phage treatment (n=4).

(C) Histopathological examination of lung tissue after phage treatment; scale bar = 100 μm. Survival curves were analyzed using the log-rank test, and other data were analyzed using two-way ANOVA. ***$p < 0.001$, **$p < 0.01$, *$p < 0.05$.

Dynamic changes in infection status of mice during phage treatment

As previously established, a phage dose of 3×10^9 PFU/mouse demonstrated substantial efficacy against lung infection. To further investigate the dynamic progression of the disease during treatment, phages were administered 1 hour post-infection, and 6 mice from each experimental group were euthanized at various time points after infection (12 h, 24 h, 48 h, and 168 h) to collect blood and lung tissue.

Over the 7-day observation period, all mice in the mock-treated group succumbed within 60 hours (Figure 5A). However, 50% of the mice in the phage-treated group survived by the end of the observation period (168 hours). These findings align with our previous studies, demonstrating that phage qsb1 therapy can significantly improve survival rates in mice suffering from acute pneumonia infected of A.baumannii. CBC results (Figure 5B) indicated a continuous rise in white blood cell counts over the first 48 hours, suggesting the progression of inflammation. besides, the TNF-α levels in the phage-treated group were significantly lower than those in the model control group (Figure 5E). These findings indicate that phage treatment effectively mitigated the inflammatory response in the lungs.

The results of lung homogenate colony counts showed that, The bacterial colonization in the lungs of mice in the mock treatment group remained at a high level(10^8 to 10^{10} CFU/g) (Figure 5C). In contrast, bacterial colonization in the phage-treated group was significantly lower at all time points. By the 48-hour mark, bacterial colonization in the phage-treated group had decreased to just 10^6 CFU/g.

Additionally, the phage titer in the lungs of the Phage-treated group was monitored during infection (Figure 5D). At 12 hours after infection, the phage titer was 10^6 PFU/g. Over time, the phage titer steadily increased, corresponding with bacterial colonization, as the phages continued to infect and alleviate infection symptoms. By 168 hours, the phage titer had reached 10^{10} PFU/g, indicating continuous phage activity in combating infection and without being cleared by the immune system.

Finally, histopathological examination of lung tissue (Figure 5F) revealed that , as the infection progressed, severe lung damage became apparent, including congestion, necrosis, inflammatory cytokine infiltration, and extensive destruction of the alveolar structure. In the Phage-treated group, only minor alveolar edema and limited inflammatory infiltration were observed at all time points, with alveolar structures remaining largely intact, and no signs of congestion, necrosis, or other severe pathological changes.

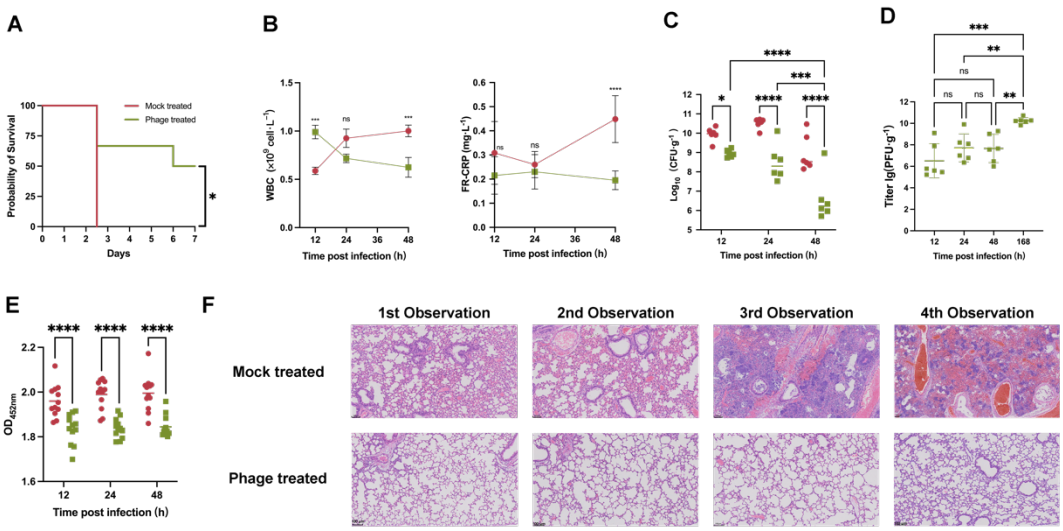

Figure 5: High-dose phage treatment in mice with *A.baumannii* lung infection.
Saline (red circles) and qsb1 phage (green squares) were administered 1 hour post-infection with *A.baumannii*. The 1st, 2nd, and 3rd observations correspond to 12h, 24h, and 48h, respectively. The 4th observation is at 60h for the Mock treated group (all mice died by 60h) and 128h for the Phage treated group.
(A) Seven-day survival curve for mice after high-dose phage treatment (n=6): Mock-treated group (red) and Phage-treated group (green). The survival rate (50%) in the phage-treated group was significantly higher than that in the Mock-treated group at the end of treatment.
(B) Changes in blood cell counts (WBC and CRP) over the course of treatment (n=6).
(C) Bacterial CFU) in the lungs of mice; each symbol represents an individual mouse, and lines represent the mean. Data represent pooled results from independent experiments, with n = 6 mice per group per time point, normalized to lung weight. The CFU in the lungs of the phage-treated group showed significant or highly significant reductions at all time points compared with the Mock-treated group.
(D) PFU in the lungs of phage-treated mice. Each symbol represents a logarithmic value, and lines represent the mean. Results represent pooled data from independent experiments, with n = 6 mice per time point, normalized to lung weight.Significant differences in PFU in the lungs were observed at the end of mouse treatment (168 h) and at other time points (12 h, 24 h, and 48 h).
(E) TNF-α levels in mouse lungs; n = 6 mice per group per time point, with two replicates per mouse. Lines represent the mean. Significant differences in TNF-α levels were observed between the Phage-treated and Mock-treated groups at all time points.
(F) Histopathological analysis of lung tissue; scale bar = 100 μm. Survival curves were analyzed using the log-rank test, while other data were analyzed using two-way ANOVA. ***$p < 0.001$, **$p < 0.01$, *$p < 0.05$.

Discussion

The global rise of antimicrobial resistance (AMR) poses a serious public health threat[22, 23]. Phage therapy, recognized for its antibacterial properties[11], offers distinct advantages over conventional treatments, including targeted activity, safety, and without disturbing the commensal microbiota[24]. Recent high-profile clinical

cases and ongoing trials in countries like the U.S., France, and Sweden underscore its potential in combating multidrug-resistant (MDR) pathogens[25].

In this study, we isolated and characterized the bacteriophage vB_AbaS_qsb1, a virulent phage with potent lytic activity against *A.baumannii*. vB_AbaS_qsb1 demonstrated remarkable stability across a broad temperature (10-60°C) and pH range (pH 3-11), indicating its potential for use under diverse physiological conditions. The phage's short latent period allows rapid bacterial lysis, despite its moderate burst size. These findings will support vB_AbaS_qsb1 as a promising candidate for therapeutic infection of *A.baumannii.*

Genome analysis of vB_AbaS_qsb1 placed it within the *Caudoviricetes* family. Despite harboring the integrase gene (CDS_1) associated with lysogeny, experimental results and lifestyle prediction analyses demonstrated that vB_AbaS_qsb1 retained characteristics of virulent phage. Moreover, this potential lysogeny gene presents an avenue for further research in gene editing. Notably, the qsb1 genome encodes a depolymerase (CDS_12), which may contribute to the phage's ability to degrade extracellular polysaccharides, a property that has garnered interest for its potential anti-biofilm and anti-infective applications [26]-[27]. Further studies are needed to explore the interaction between vB_AbaS_qsb1 depolymerase and *A.baumannii.*

Safety is a critical factor in the clinical use of phage therapy[27]. In this study, intratracheal administration of 10^9 PFU vB_AbaS_qsb1 to mice did not induce adverse clinical symptoms, with stable inflammatory markers and no significant lung tissue damage. These results confirm the safety of vB_AbaS_qsb1, essential for its clinical advancement. Moreover, further in vivo experiments demonstrated its therapeutic efficacy, phage significantly reducing bacterial loads of lung and improving survival rates in mice with *A.baumannii* lung infections. The phages persisted in the lungs for up to a week post-treatment without immune system clearance, continuously reducing bacterial load while proliferating. This, combined with their host specificity and minimal impact on beneficial microbiota, highlights their potential as an effective alternative against multidrug-resistant bacterial infections.

While our results are promising, several limitations remain. The efficacy of vB_AbaS_qsb1 in chronic infections hosts warrants further study. Additionally, the survival rate of treated mice, although improved, remained at 50%. This may be attributed to mechanical damage during phage administration or the empirical nature of current phage therapy protocols[28, 29]. Therefore, future studies can further evaluate the impact of different administration routes of phage on the survival rate of mice while ensuring safety. Finally, in addition to the route of administration, it is worth further study on whether to use a single phage or a phage cocktail, phage dosage and endotoxin levels in phage preparations, frequency and time of administration, and phage neutralizing antibodies.

In conclusion, we successfully isolated and characterized a novel *A.baumannii* virulent phage, vB_AbaS_qsb1. This phage exhibited potent lytic activity both in vitro and in vivo, demonstrating its ability to effectively eliminate *A. baumannii*, highlighting its potential as a promising therapeutic agent. Additionally, this phage exhibited a favorable safety profile in animal models, with treatment using qsb1 rescuing over 50%

of mice with acute *A.baumannii* pneumonia. Notably, qsb1 maintained high phage titers in the lungs 7 days post-administration, which may also indicate that qsb1 has certain potential in the preventive treatment of *A.baumannii* infection. As antibiotic resistance continues to rise, phage therapy holds great promise as an alternative or adjunct to traditional antimicrobial treatments.

2 Material and method

2.1 Bacterial strains and culture conditions

A.baumannii ioag01 was obtained from our laboratory in a previous study[30]. In this study, *ioag01* was used as a host strain to isolate phages. The frozen bacteria were first streaked on Luria-Bertani Broth for 12 h (37 ℃), and then single colonies were picked and enriched in liquid culture medium in a constant temperature shaking incubator at 220 rpm (37 ℃, 12 h). The bacterial culture was stored at -80 ℃ for long-term with 10% glycerol as a cryoprotectant.

2.2 Phage isolation and purification

Water samples were collected from the lake in Qishan Lake Park, Fuzhou City, Fujian Province, China. The samples were centrifuged and filtered through a 0.22 μm PES membrane filter. The filtrate was collected in a sterile centrifuge tube. For the enrichment of bacteriophages, the bacterial culture (*A.baumannii ioag01*) was first centrifuged and the supernatant was removed. The bacterial precipitate was resuspended in the 2× LB liquid medium and an equal volume of filtrate was added to it. The mixture was co-cultured at 220 rpm (37 ℃, 5~7 d). The mixture solution was then centrifuged at 20,000 g (4 ℃, 10 min). The supernatant was collected and the presence of phages was detected by the drop method[31].For positive samples detected by the drop method, the phage suspension was first serially diluted using SM buffer (1.972 g/L $MgSO_4 \cdot 7H_2O$, 5.85 g/L NaCl, 50 mL/L 1M Tris-HCl（pH 7.5）, 5.0 mL/L 2% Gelatin). Subsequently, 500 μL of the phage dilution was mixed with 500 μL of bacterial culture and incubated at 37 ℃ for 10 minutes. The 1 mL mixture was then added to 0.6% semi-solid medium and layered onto the surface of a 1.5% solid medium to form double-layer plates, which were incubated overnight at 37 ℃. Individual plaques were picked into SM buffer on the second day. To purify the isolated phage, an individual plaque was picked and passaged at 3~5 times by the double-layer agar (DLA) method. Single plaques were collected to complete the purification and determine the phage titer.

2.3 Phage amplification, concentration, and storage

A 500 μL aliquot of the purified phage lysate was mixed with 500 μL of bacterial culture and incubated overnight at 37 ℃. The mixture was then centrifuged at 20,000 g (4 ℃, 10 min). The phage-containing supernatant was collected and added to 5 mL of bacterial culture. This mixture was incubated at 220 rpm (37 ℃) until the culture became clear. Subsequently, the culture was centrifuged again at 20,000 g (4 ℃, 10 min). The supernatant was filtered through a 0.22 μm PES membrane to obtain the phage suspension. The phage suspension was then mixed with a 4× virus concentration solution (400 g/L PEG-8000, 70 g/L NaCl, 100 mL/L 10× PBS buffer, pH 6.8) at a 3:1

405 (v/v) ratio and allowed to stand at 4 ℃ overnight. Following this, the mixture was
406 centrifuged at 12,000 g (4 ℃, 15 min), and the supernatant was discarded. The phage
407 pellet was resuspended in SM buffer. Finally, the phage particles were stored at -80 ℃
408 using 10 mg/mL PEG-4000 as a cryoprotectant for long-term preservation.

409 **2.4 Transmission electron microscopy (TEM)**

410 A 20 μL aliquot of the concentrated phage particle suspension was applied to the surface
411 of a carbon-coated copper grid and allowed to stand for 10 minutes. Excess liquid was
412 then removed using filter paper. The grid was subsequently stained with 20 μL of 2%
413 phosphotungstic acid for 90 seconds to achieve negative staining. After removing the
414 excess stain with filter paper, the grid was left to dry overnight. Imaging was performed
415 using a transmission electron microscope (TEM, HT7800, HITACHI) operating at an
416 accelerating voltage of 100 kV.

417 **2.5 Multiplicity of infection (MOI) of phages**

418 The concentration of the host bacterial culture was determined by turbidimetry, and the
419 bacterial concentration was adjusted to 10^8 CFU/mL. The titer of phage qsb1 was then
420 determined using the DLA method. Phage and host bacterial cultures were mixed in
421 equal volumes at MOI of 0.01, 0.1, 1, 10, and 100, and incubated with shaking at 220
422 rpm (37 ℃, 6 h). Following incubation, the cultures were centrifuged, and the phage
423 titer was measured. Three independent experiments were performed.

424 **2.6 One-Step growth curve of phages**

425 The phage and host bacterial culture were mixed at the optimal multiplicity of infection
426 (MOI=0.1) determined previously, and incubated at 37 ℃ for 10 minutes. The
427 supernatant was then discarded, and the precipitate was washed once with LB liquid
428 medium by centrifugation at 20,000 g (4 ℃, 1 min). The precipitate was resuspended
429 in LB medium and incubated with shaking at 220 rpm (37 ℃, 4h). Samples were
430 collected every 20 minutes during the first 2 hours, and every 30 minutes during the
431 final 2 hours, for phage titer determination. Three independent experiments were
432 performed.

433 **2.7 Temperature and pH stability of phages**

434 To assess the temperature stability of phage qsb1, a phage suspension with a previously
435 measured titer was incubated at temperatures of 10 ℃, 20 ℃, 40 ℃, 60 ℃, 80 ℃, and
436 100 ℃ for 30, 60, and 90 minutes, respectively, followed by phage titer determination.
437 Three independent experiments were performed.
438 Similarly, to evaluate the pH stability of phage qsb1, 100 μL of phage suspension (with
439 a known titer) was mixed with 900 μL of SM buffer at various pH levels (1, 3, 5, 7, 8,
440 9, 11, 13) and incubated (4 ℃,1 h). Subsequently, the pH of the mixtures was adjusted
441 with appropriate amounts of NaOH or HCl to a level suitable for bacterial growth, and
442 the phage titer was measured. Three independent experiments were performed.

443 **2.8 Extraction, sequencing, and analysis of phage genomes**

444 The total genome of the phage was extracted using the phenol-chloroform method, with
445 nuclease digestion performed beforehand to eliminate host bacterial nucleic acids from
446 the sample. The concentration of the extracted genome was measured using a Nanodrop
447 2000 spectrophotometer (Thermo Fisher Scientific). The genome was treated with
448 RNase A (Gproan, GPE007001), DNase I (Thermo Fisher Scientific, EN0521), and S1

nucleases (Thermo Fisher Scientific, EN0321) to confirm its nucleic acid type and structural integrity. Subsequently, Pulsed-Field Gel Electrophoresis(Pippin-pluse，sage science) was employed to confirm the size of the phage genome nucleic acid.Next-generation sequencing (NGS) library of the phage genome was constructed using the Nextera library preparation kit, followed by high-throughput sequencing on the Illumina NovaSeq™ X Plus system.

Post-sequencing, quality control of the raw data was conducted to ensure high-quality reads, which were then assembled using MEGAHIT software[32]. For functional annotation of the assembled phage sequences, several bioinformatics tools were utilized, including Prokka[33],RAST[34], GeneMarks[35], Phagescope[36],and Phastest[37]. Phage lifestyle prediction was conducted using the DeepPhage[38] tool to determine whether the isolated phage exhibits a lytic or lysogenic lifecycle.The integrated gene annotation results provided comprehensive genomic information for the phage qsb1. Genomic features were visualized using the CGView[39] online server. A phylogenetic tree for phage qsb1 was constructed using MEGA X software[40], with further aesthetic enhancements made using the Chiplot tool[41]. For comparative analysis of whole-genome collinearity among phages, RStudio[42] with the gggenomes package[43] was employed to generate a whole-genome comparison visualization map.

2.9 Mice

For all mouse experiments, we selected male BALB/C mice aged 6-8 weeks. Upon arrival at the facility, the mice randomly were housed in clean individually ventilated cages (IVC) with 5-6 mice per group, Random numbers were generated using the standard = RAND() function in Microsoft Excel. All mice were used after a 7-day acclimatization period. They were fed with irradiated sterilized feed and provided distilled water sterilized by high-pressure wet heat. The housing conditions were maintained at a constant temperature of 24-26 ℃, humidity of 50%-60%, with a 12-hour light/dark cycle.

2.10 Preparation of bacterial culture and phage suspension

The bacterial culture of *A.baumannii* was prepared as described in section 2.1, with the concentration adjusted by turbidimetry. A 1 mL aliquot of the bacterial culture was centrifuged at 20,000 g (4 ℃, 10 min), and the pellet was collected. The pellet was washed with 0.9% NaCl, and then resuspended in 30 μL of 0.9% NaCl for use. Bacteria were removed from the phage suspension using a 0.22 μm microporous membrane, and the phage titer was subsequently determined using the DLA method. Subsequently, the phage suspension was centrifuged at 100,000 g (4 ℃, 2 h). The phage pellet was resuspended in 0.9% NaCl to a final concentration of 1×10^{12} PFU/mL for further use.

2.11 Establishment of a mouse pneumonia model via intratracheal instillation

In previous studies, tracheal access often involved surgical procedures to locate the trachea for drug administration or model establishment, which could introduce experimental variability, such as post-surgical infections or complications during the procedure. To mitigate these risks, we employed a Non-invasive intratracheal instillation approach to construct the mouse pneumonia model [44]. This method is straightforward, rapid, and effective. The anesthetized mouse was positioned supine on

an intubation platform, with the head secured, and a disposable indwelling needle was inserted into the glottis using a small animal laryngoscope to complete the endotracheal intubation.

2.12 The model of pulmonary infection caused by *A.baumannii* in mice and phage safety

To induce neutropenia and simulate the immunocompromised state of clinical patients, mice were intraperitoneally injected with cyclophosphamide(CTX) at doses of 200 mg/kg and 150 mg/kg, 4 days and 1 day prior to infection, respectively. In previous studies, a bacterial dose ranging from $10^8 \sim 10^9$ CFU was commonly used to establish an acute pulmonary bacterial infection model in mice[45]. In this study, mice were anesthetized and inoculated via tracheal instillation with varying doses of *A. baumannii ioag01* (3×10^9 CFU/mouse, 3×10^8 CFU/mouse, 3×10^7 CFU/mouse, 3×10^6 CFU/mouse). In the phage-treated group, mice were administered 1×10^9 PFU/mouse of phage qsb1 via tracheal instillation, while the control group received an equivalent volume of 0.9% NaCl. Mice were observed for seven days, and survival rates were recorded to determine the median lethal dose (LD50) of the bacteria and to evaluate the safety of the phage treatment.

2.13 Phage treatment for acute pulmonary infection caused by *A.baumannii* in mice

After determining the appropriate bacterial dose (3×10^8 CFU/mouse) for the mouse lung infection model, phages were used to treat the infected mice to assess therapeutic efficacy. Twenty-five BALB/C mice were randomly divided into five groups. They were intraperitoneally injected with 200 mg/kg and 150 mg/kg of CTX, 4 days and 1 day before infection, respectively. Mice were anesthetized and infected with 3×10^8 CFU of *A.baumannii ioag01*. One hour post-infection, 30 μL of 0.9% NaCl was administered by tracheal instillation (mock-treated group). The experimental groups received varying phage titers (3×10^9 PFU, high-dose; 3×10^8 PFU, medium-dose; and 3×10^7 PFU, low-dose). The control group received 30 μL of 0.9% NaCl initially, and an additional 30 μL of 0.9% NaCl one hour later to control for procedural variables. All mice were observed for seven days, during which their conditions and mortality were recorded.

2.14 High-Dose phage treatment for acute pulmonary infection caused by *A.baumannii* in mice

To further evaluate the pathological changes during infection and the therapeutic effect of high-dose phage treatment, 48 BALB/C mice were randomly divided into two groups. They were injected intraperitoneally with 200 mg/kg and 150 mg/kg of CTX, 4 days and 1 day prior to infection, respectively. After anesthesia, a lung infection model was established as previously described. One hour after bacterial infection, the experimental group received 3×10^9 PFU of phage by tracheal instillation, while the control group received 30 μL of 0.9% NaCl. Subsequently, six mice were euthanized by cervical dislocation at 12、24、48 and 168 hours post-infection. Whole blood and lung tissues were collected aseptically from each mouse. Whole blood and lung tissues were collected under sterile conditions. CBC were conducted to evaluate systemic responses, while bacterial and phage colonization in the lungs was assessed by homogenizing the right lung. The left lung was fixed in paraformaldehyde and stained with hematoxylin-

eosin (HE) to assess lung pathology.

2.15 Determination of bacterial and phage colonization

After the mice were sacrificed, their lungs were aseptically removed, weighed, and mechanically homogenized in PBS containing protease inhibitors (PMSF). The lung homogenates were kept on ice and serially diluted within 1 hour. The bacterial load (CFU) in the lungs was quantified using standard microbiological methods, while the phage titer (PFU) of bacteriophage qsb1 was determined using the DLA method. Finally, the unit is CFU/g or PFU/g.

2.16 Cytokine quantification

For the treated lung tissue homogenate, the concentrations of interleukins (IL-1β, IL-6) and tumor necrosis factor-α (TNF-α) were quantified using ELISA. Cytokine levels were expressed the total protein relative content in the lung homogenate, measured as the optical density at 450 nm (OD_{450nm}).

2.16 Complete blood count

After collecting whole blood from the mice, blood parameters were analyzed within 1 hour using an automated blood cell counter (XN-550,Sysmex America).

2.17 Histopathological Analysis

Following euthanasia, lung tissues were harvested and immediately fixed in 4% paraformaldehyde. The fixed tissues were processed for dehydration using an automated tissue dehydration processor (HistoCore PEGASUS, Leica), embedded in paraffin (HistoCore Arcadia H&C, Leica), and sectioned into 4 μm thick slices using a microtome (HistoCore Multicut, Leica). Sections were stained with hematoxylin and eosin (H&E) utilizing an automated staining system (HistoCore CHROMAX ST, Leica) and coverslipped with an automated coverslipper (Leica CV5030). Digital images of the stained sections were acquired and analyzed using a digital pathology slide scanner (KF-PRO-005-EX, KFBIO).

Statistical analysis.

Data were evaluated using two-way ANOVA or the log-rank test for survival curves, unless otherwise indicated. A p-value of ≤0.05 was considered statistically significant.

Transparency declaration

Conflict of interest

The bacteriophage strain vB_AbaS_qsb1 has been filed for a patent.

Funding

Natural fund project of Fujian Province, China (No. 2024J011223); Fuzhou Health science and technology plan soft science research project (No. 2022-S-wr4); Young and middle-aged talent research project of Fuzhou city(No. 2022-S-rc5);National Key Research & Development Plan (No. 2023YFC3304304);Fuzhou University Testing Fund of precious apparatus (No. 2024T021); Fujian Provincial Science and Technology Plan Project ((No. 2022Y4003); National Key Research & Development Plan ((No. 2023YFC3304304). Fujian Provincial Major Health Research Project (grant number

2022ZD01001)

Data availability

The datasets generated during and/or analyzed during the current study are available from the corresponding author on reasonable request. All other data supporting the findings of this study are included within the article and its supplementary materials.

Author contributions

J.L. and X.Y. jointly conceived the study design. J.W., Q.W., T.Z., X.R., and W.J. performed the experiments and contributed to data interpretation. J.W. conducted all data analyses and drafted the manuscript. J.L., X.Y., and X.H. critically reviewed and provided final approval of the manuscript.

Ethical statement

All protocols in this study were approved by the Committee on the Ethics of Animal Experiments of College of Biological Science and Engineering, Fuzhou University (the authority of the project licence: KS2023-SG-042)

Declaration of Generative AI and AI-assisted technologies in the writing process

During the preparation of this work the author(s) used Chat-GPT 4o in order to improve the language and readability,with caution. After using this tool, the authors reviewed and edited the content as needed and take full responsibility for the content of the publication.

Reference

[1] A. Bianco, A. Quirino, M. Giordano, V. Marano, C. Rizzo, M.C. Liberto, et al., Control of carbapenem-resistant Acinetobacter baumannii outbreak in an intensive care unit of a teaching hospital in Southern Italy, BMC Infect Dis 16(1) (2016) 747.http://doi.org/10.1186/s12879-016-2036-7

[2] C. Ayoub Moubareck, D. Hammoudi Halat, Insights into Acinetobacter baumannii: A Review of Microbiological, Virulence, and Resistance Traits in a Threatening Nosocomial Pathogen, Antibiotics (Basel) 9(3) (2020).http://doi.org/10.3390/antibiotics9030119

[3] T.A. Hafiz, S.S. Alghamdi, M.A. Mubaraki, S.S.M. Alghamdi, A. Alothaybi, E. Aldawood, et al., A two-year retrospective study of multidrug-resistant Acinetobacter baumannii respiratory infections in critically Ill patients: Clinical and microbiological findings, J Infect Public Health 16(3) (2023) 313-319.http://doi.org/10.1016/j.jiph.2023.01.004

[4] S. Mohd Sazlly Lim, A. Zainal Abidin, S.M. Liew, J.A. Roberts, F.B. Sime, The global prevalence of multidrug-resistance among Acinetobacter baumannii causing hospital-acquired and ventilator-associated pneumonia and its associated mortality: A systematic review and meta-analysis, J Infect 79(6) (2019) 593-600.http://doi.org/10.1016/j.jinf.2019.09.012

[5] M.S. Mulani, E.E. Kamble, S.N. Kumkar, M.S. Tawre, K.R. Pardesi, Emerging Strategies to Combat ESKAPE Pathogens in the Era of Antimicrobial Resistance: A Review, Front Microbiol 10 (2019) 539.http://doi.org/10.3389/fmicb.2019.00539

[6] M. Vestergaard, W. Paulander, R.L. Marvig, J. Clasen, N. Jochumsen, S. Molin, et al., Antibiotic combination therapy can select for broad-spectrum multidrug resistance in Pseudomonas aeruginosa, Int J Antimicrob Agents 47(1) (2016) 48-55.http://doi.org/10.1016/j.ijantimicag.2015.09.014

[7] N.M. Clark, G.G. Zhanel, J.P. Lynch, 3rd, Emergence of antimicrobial resistance among Acinetobacter species: a global threat, Curr Opin Crit Care 22(5) (2016) 491-

9.http://doi.org/10.1097/MCC.0000000000000337
[8] P. Gallagher, S. Baker, Developing new therapeutic approaches for treating infections caused by multi-drug resistant Acinetobacter baumannii: Acinetobacter baumannii therapeutics, J Infect 81(6) (2020) 857-861.http://doi.org/10.1016/j.jinf.2020.10.016
[9] WHO publishes list of bacteria for which new antibiotics are urgently needed. <https://www.who.int/news-room/detail/27-02-2017-who-publishes-list-of-bacteria-for-which-new-antibiotics-are-urgently-needed>, 2017 GENEVA).
[10] WHO updates list of drug-resistant bacteria most threatening to human health. <https://www.who.int/zh/news/item/17-05-2024-who-updates-list-of-drug-resistant-bacteria-most-threatening-to-human-health>, 2024 Geneva).
[11] G.P. Salmond, P.C. Fineran, A century of the phage: past, present and future, Nat Rev Microbiol 13(12) (2015) 777-86.http://doi.org/10.1038/nrmicro3564
[12] P. Domingo-Calap, J. Delgado-Martinez, Bacteriophages: Protagonists of a Post-Antibiotic Era, Antibiotics (Basel) 7(3) (2018).http://doi.org/10.3390/antibiotics7030066
[13] M. Jamal, S. Andleeb, F. Jalil, M. Imran, M.A. Nawaz, T. Hussain, et al., Isolation, characterization and efficacy of phage MJ2 against biofilm forming multi-drug resistant Enterobacter cloacae, Folia Microbiol (Praha) 64(1) (2019) 101-111.http://doi.org/10.1007/s12223-018-0636-x
[14] M. Dvorackova, F. Ruzicka, M. Benesik, R. Pantucek, M. Dvorakova-Heroldova, Antimicrobial effect of commercial phage preparation Stafal(R) on biofilm and planktonic forms of methicillin-resistant Staphylococcus aureus, Folia Microbiol (Praha) 64(1) (2019) 121-126.http://doi.org/10.1007/s12223-018-0622-3
[15] E.A. Ashworth, R.C.T. Wright, R.K. Shears, J.K.L. Wong, A. Hassan, J.P.J. Hall, et al., Exploiting lung adaptation and phage steering to clear pan-resistant Pseudomonas aeruginosa infections in vivo, Nat Commun 15(1) (2024) 1547.http://doi.org/10.1038/s41467-024-45785-z
[16] R.Y.K. Chang, M.Y.T. Chow, Y. Wang, C. Liu, Q. Hong, S. Morales, et al., The effects of different doses of inhaled bacteriophage therapy for Pseudomonas aeruginosa pulmonary infections in mice, Clin Microbiol Infect 28(7) (2022) 983-989.http://doi.org/10.1016/j.cmi.2022.01.006
[17] J.A. Nick, R.M. Dedrick, A.L. Gray, E.K. Vladar, B.E. Smith, K.G. Freeman, et al., Host and pathogen response to bacteriophage engineered against Mycobacterium abscessus lung infection, Cell 185(11) (2022) 1860-1874 e12.http://doi.org/10.1016/j.cell.2022.04.024
[18] M. Bernabeu-Gimeno, M. Pardo-Freire, B.K. Chan, P.E. Turner, A. Gil-Brusola, S. Perez-Tarazona, et al., Neutralizing antibodies after nebulized phage therapy in cystic fibrosis patients, Med (2024).http://doi.org/10.1016/j.medj.2024.05.017
[19] R.T. Schooley, B. Biswas, J.J. Gill, A. Hernandez-Morales, J. Lancaster, L. Lessor, et al., Development and Use of Personalized Bacteriophage-Based Therapeutic Cocktails To Treat a Patient with a Disseminated Resistant Acinetobacter baumannii Infection, Antimicrob Agents Chemother 61(10) (2017).http://doi.org/10.1128/AAC.00954-17
[20] R. Nir-Paz, D. Gelman, A. Khouri, B.M. Sisson, J. Fackler, S. Alkalay-Oren, et al., Successful Treatment of Antibiotic-resistant, Poly-microbial Bone Infection With Bacteriophages and Antibiotics Combination, Clin Infect Dis 69(11) (2019) 2015-2018.http://doi.org/10.1093/cid/ciz222
[21] S. Federici, S. Kredo-Russo, R. Valdes-Mas, D. Kviatcovsky, E. Weinstock, Y. Matiuhin, et al., Targeted suppression of human IBD-associated gut microbiota commensals by phage consortia for treatment of intestinal inflammation, Cell 185(16) (2022) 2879-2898 e24.http://doi.org/10.1016/j.cell.2022.07.003

[22] W.h. organization, Report signals increasing resistance to antibiotics in bacterial infections in humans and need for better data. <https://www.who.int/zh/news/item/09-12-2022-report-signals-increasing-resistance-to-antibiotics-in-bacterial-infections-in-humans-and-need-for-better-data>, 2024 Geneva).
[23] C.J.L. Murray, K.S. Ikuta, F. Sharara, L. Swetschinski, G. Robles Aguilar, A. Gray, et al., Global burden of bacterial antimicrobial resistance in 2019: a systematic analysis, The Lancet 399(10325) (2022) 629-655.http://doi.org/10.1016/s0140-6736(21)02724-0
[24] Y. Ali, I. Inusa, G. Sanghvi, V.B. Mandaliya, A.K. Bishoyi, The current status of phage therapy and its advancement towards establishing standard antimicrobials for combating multi drug-resistant bacterial pathogens, Microbial Pathogenesis 181 (2023).http://doi.org/10.1016/j.micpath.2023.106199
[25] S.A. Strathdee, G.F. Hatfull, V.K. Mutalik, R.T. Schooley, Phage therapy: From biological mechanisms to future directions, Cell 186(1) (2023) 17-31.http://doi.org/10.1016/j.cell.2022.11.017
[26] M. Li, H. Wang, L. Chen, G. Guo, P. Li, J. Ma, et al., Identification of a phage-derived depolymerase specific for KL47 capsule of Klebsiella pneumoniae and its therapeutic potential in mice, Virol Sin 37(4) (2022) 538-546.http://doi.org/10.1016/j.virs.2022.04.005
[27] Y. Liu, S.S.Y. Leung, Y. Huang, Y. Guo, N. Jiang, P. Li, et al., Identification of Two Depolymerases From Phage IME205 and Their Antivirulent Functions on K47 Capsule of Klebsiella pneumoniae, Front Microbiol 11 (2020) 218.http://doi.org/10.3389/fmicb.2020.00218
[28] G. Mitropoulou, A. Koutsokera, C. Csajka, S. Blanchon, A. Sauty, J.F. Brunet, et al., Phage therapy for pulmonary infections: lessons from clinical experiences and key considerations, Eur Respir Rev 31(166) (2022).http://doi.org/10.1183/16000617.0121-2022
[29] Q. Hong, R.Y.K. Chang, O. Assafiri, S. Morales, H.K. Chan, Optimizing in vitro phage-ciprofloxacin combination formulation for respiratory therapy of multi-drug resistant Pseudomonas aeruginosa infections, Int J Pharm 652 (2024) 123853.http://doi.org/10.1016/j.ijpharm.2024.123853
[30] J. Lin, W. Jiang, Y. Shi, W. Cai, Metagenomic Sequencing Revealed the Potential Pathogenic Threats of Banknotes, ACS Omega 6(5) (2021) 3499-3507.http://doi.org/10.1021/acsomega.0c04546
[31] N. Acs, M. Gambino, L. Brondsted, Bacteriophage Enumeration and Detection Methods, Front Microbiol 11 (2020) 594868.http://doi.org/10.3389/fmicb.2020.594868
[32] D. Li, C.-M. Liu, R. Luo, K. Sadakane, T.-W. Lam, MEGAHIT: an ultra-fast single-node solution for large and complex metagenomics assembly via succinct de Bruijn graph, Bioinformatics 31(10) (2015) 1674-1676.http://doi.org/10.1093/bioinformatics/btv033
[33] T. Seemann, Prokka: rapid prokaryotic genome annotation, Bioinformatics 30(14) (2014) 2068-2069.http://doi.org/10.1093/bioinformatics/btu153
[34] R.K. Aziz, D. Bartels, A.A. Best, M. DeJongh, T. Disz, R.A. Edwards, et al., The RAST Server: Rapid Annotations using Subsystems Technology, BMC Genomics 9(1) (2008).http://doi.org/10.1186/1471-2164-9-75
[35] J. Besemer, GeneMarkS: a self-training method for prediction of gene starts in microbial genomes. Implications for finding sequence motifs in regulatory regions, Nucleic Acids Research 29(12) (2001) 2607-2618.http://doi.org/10.1093/nar/29.12.2607
[36] R.H. Wang, S. Yang, Z. Liu, Y. Zhang, X. Wang, Z. Xu, et al., PhageScope: a well-annotated bacteriophage database with automatic analyses and visualizations, Nucleic Acids Res 52(D1) (2024) D756-D761.http://doi.org/10.1093/nar/gkad979
[37] D.S. Wishart, S. Han, S. Saha, E. Oler, H. Peters, J.R. Grant, et al., PHASTEST: faster than PHASTER, better than PHAST, Nucleic Acids Res 51(W1) (2023) W443-

W450.http://doi.org/10.1093/nar/gkad382
[38] S. Wu, Z. Fang, J. Tan, M. Li, C. Wang, Q. Guo, et al., DeePhage: distinguishing virulent and temperate phage-derived sequences in metavirome data with a deep learning approach, GigaScience 10(9) (2021).http://doi.org/10.1093/gigascience/giab056
[39] J.R. Grant, E. Enns, E. Marinier, A. Mandal, E.K. Herman, C.Y. Chen, et al., Proksee: in-depth characterization and visualization of bacterial genomes, Nucleic Acids Res 51(W1) (2023) W484-W492.http://doi.org/10.1093/nar/gkad326
[40] S. Kumar, G. Stecher, M. Li, C. Knyaz, K. Tamura, MEGA X: Molecular Evolutionary Genetics Analysis across Computing Platforms, Mol Biol Evol 35(6) (2018) 1547-1549.http://doi.org/10.1093/molbev/msy096
[41] J. Xie, Y. Chen, G. Cai, R. Cai, Z. Hu, H. Wang, Tree Visualization By One Table (tvBOT): a web application for visualizing, modifying and annotating phylogenetic trees, Nucleic Acids Res 51(W1) (2023) W587-W592.http://doi.org/10.1093/nar/gkad359
[42] R. Team, RStudio: Integrated Development for R. <http://www.rstudio.com/>, 2020).
[43] H. T, A. M, v.A. B, gggenomes: A Grammar of Graphics for Comparative Genomics.R package version 1.0.1. <https://github.com/thackl/gggenomes>, 2024).
[44] Y. Zeng, H. Jin, J. Wang, C. Guo, W. Chen, Y. Tan, et al., An optimized method for intratracheal instillation in mice, J Pharmacol Toxicol Methods 118 (2022) 107230.http://doi.org/10.1016/j.vascn.2022.107230
[45] X. Yang, A. Haque, S. Matsuzaki, T. Matsumoto, S. Nakamura, The Efficacy of Phage Therapy in a Murine Model of Pseudomonas aeruginosa Pneumonia and Sepsis, Front Microbiol 12 (2021) 682255.http://doi.org/10.3389/fmicb.2021.682255

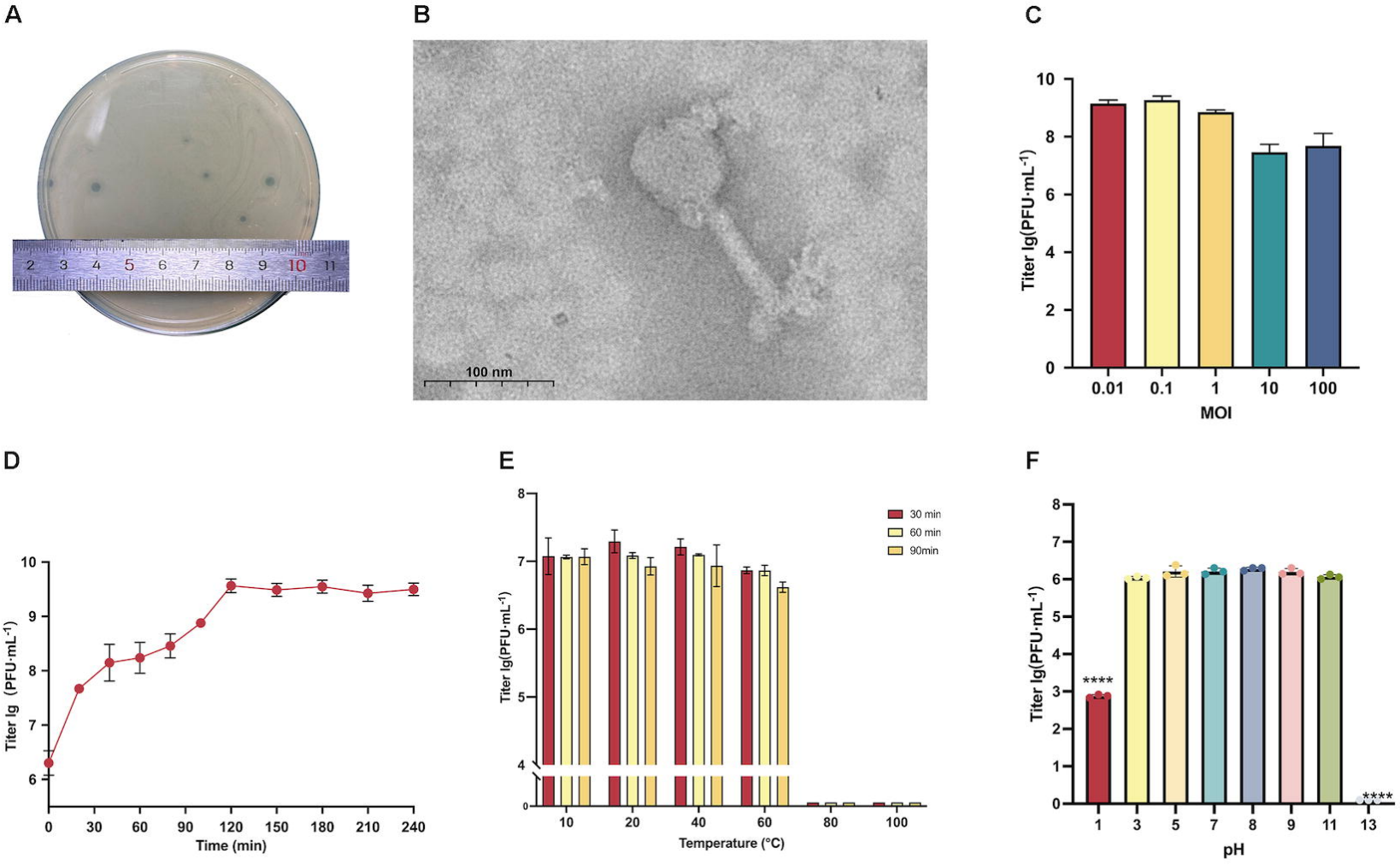
A
B
100 nm
C
Titer lg(PFU·mL-1)
MOI
0.01
0.1
1
10
100
D
Titer lg (PFU·mL-1)
Time (min)
E
30 min
60 min
90min
Titer lg(PFU·mL-1)
Temperature (°C)
F
Titer lg(PFU·mL-1)
pH
****
****

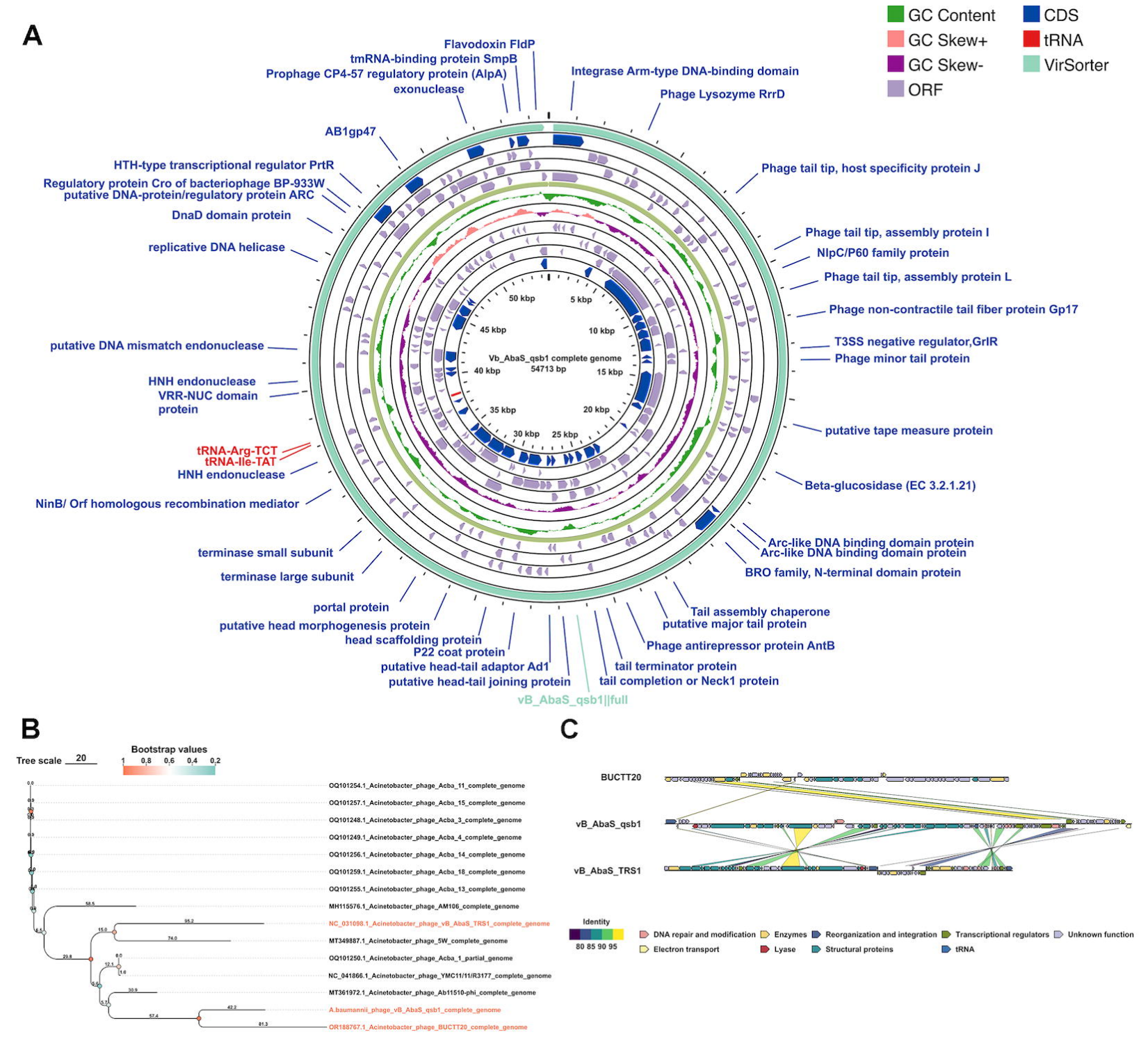
A
GC Content
GC Skew+
GC Skew-
ORF
CDS
tRNA
VirSorter
Flavodoxin FldP
tmRNA-binding protein SmpB
Prophage CP4-57 regulatory protein (AlpA)
exonuclease
Integrase Arm-type DNA-binding domain
Phage Lysozyme RrrD
AB1gp47
HTH-type transcriptional regulator PrtR
Regulatory protein Cro of bacteriophage BP-933W
putative DNA-protein/regulatory protein ARC
DnaD domain protein
replicative DNA helicase
Phage tail tip, host specificity protein J
Phage tail tip, assembly protein I
NlpC/P60 family protein
Phage tail tip, assembly protein L
Phage non-contractile tail fiber protein Gp17
T3SS negative regulator,GrlR
Phage minor tail protein
putative DNA mismatch endonuclease
HNH endonuclease
VRR-NUC domain protein
tRNA-Arg-TCT
tRNA-Ile-TAT
HNH endonuclease
NinB/ Orf homologous recombination mediator
putative tape measure protein
Beta-glucosidase (EC 3.2.1.21)
Arc-like DNA binding domain protein
Arc-like DNA binding domain protein
BRO family, N-terminal domain protein
terminase small subunit
terminase large subunit
portal protein
putative head morphogenesis protein
head scaffolding protein
P22 coat protein
putative head-tail adaptor Ad1
putative head-tail joining protein
vB_AbaS_qsb1||full
tail terminator protein
tail completion or Neck1 protein
Phage antirepressor protein AntB
Tail assembly chaperone
putative major tail protein
Vb_AbaS_qsb1 complete genome
54713 bp
5 kbp
10 kbp
15 kbp
20 kbp
25 kbp
30 kbp
35 kbp
40 kbp
45 kbp
50 kbp
B
Tree scale 20
Bootstrap values
1 0.8 0.6 0.4 0.2
OQ101254.1_Acinetobacter_phage_Acba_11_complete_genome
OQ101257.1_Acinetobacter_phage_Acba_15_complete_genome
OQ101248.1_Acinetobacter_phage_Acba_3_complete_genome
OQ101249.1_Acinetobacter_phage_Acba_4_complete_genome
OQ101256.1_Acinetobacter_phage_Acba_14_complete_genome
OQ101259.1_Acinetobacter_phage_Acba_18_complete_genome
OQ101255.1_Acinetobacter_phage_Acba_13_complete_genome
MH115576.1_Acinetobacter_phage_AM106_complete_genome
NC_031098.1_Acinetobacter_phage_vB_AbaS_TRS1_complete_genome
MT349887.1_Acinetobacter_phage_5W_complete_genome
OQ101250.1_Acinetobacter_phage_Acba_1_partial_genome
NC_041866.1_Acinetobacter_phage_YMC11/11/R3177_complete_genome
MT361972.1_Acinetobacter_phage_Ab11510-phi_complete_genome
A.baumannii_phage_vB_AbaS_qsb1_complete_genome
OR188767.1_Acinetobacter_phage_BUCTT20_complete_genome
C
BUCTT20
vB_AbaS_qsb1
vB_AbaS_TRS1
Identity
80 85 90 95
DNA repair and modification
Enzymes
Reorganization and integration
Transcriptional regulators
Unknown function
Electron transport
Lyase
Structural proteins
tRNA

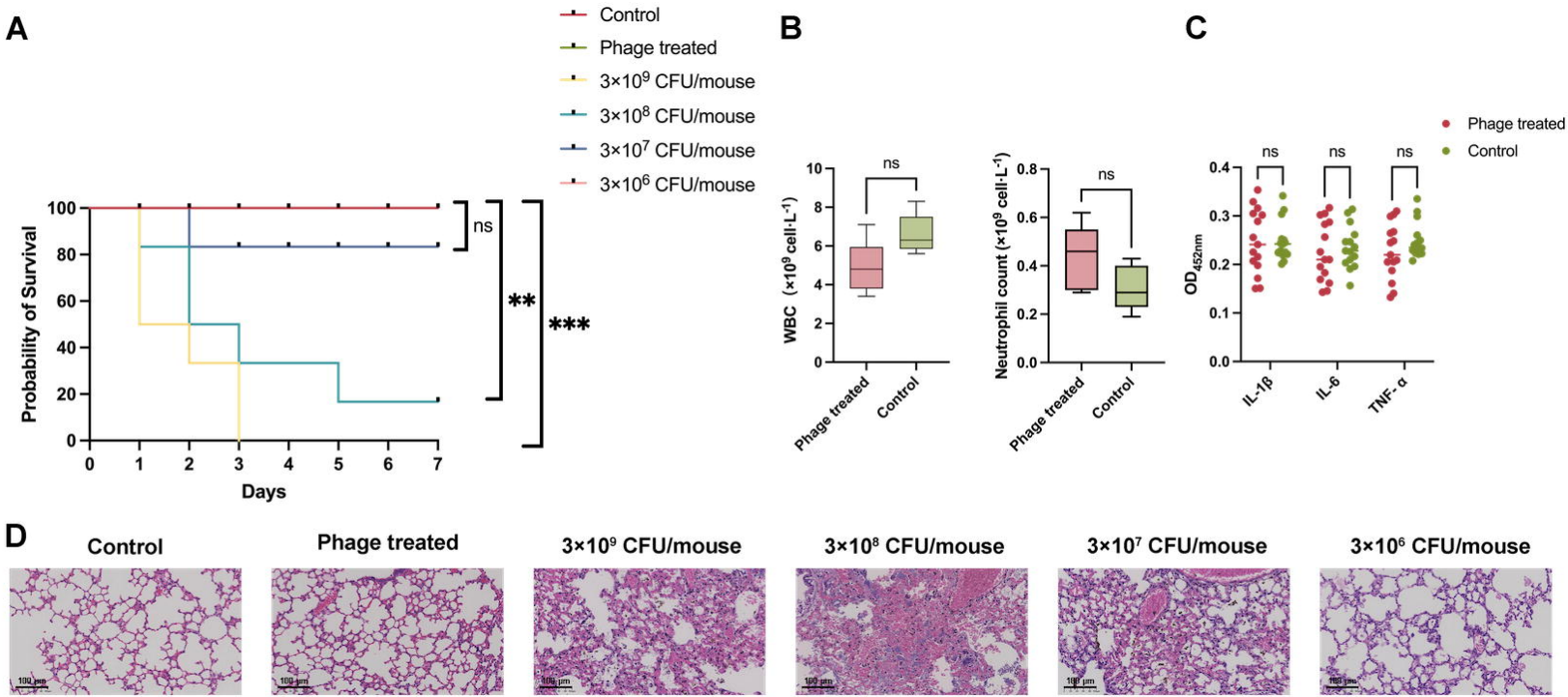
A
Control
Phage treated
3×10⁹ CFU/mouse
3×10⁸ CFU/mouse
3×10⁷ CFU/mouse
3×10⁶ CFU/mouse
Probability of Survival
Days
ns
**
***
B
WBC (×10⁹ cell·L⁻¹)
Neutrophil count (×10⁹ cell·L⁻¹)
Phage treated
Control
C
OD452nm
IL-1β
IL-6
TNF-α
D
Control
Phage treated
3×10⁹ CFU/mouse
3×10⁸ CFU/mouse
3×10⁷ CFU/mouse
3×10⁶ CFU/mouse

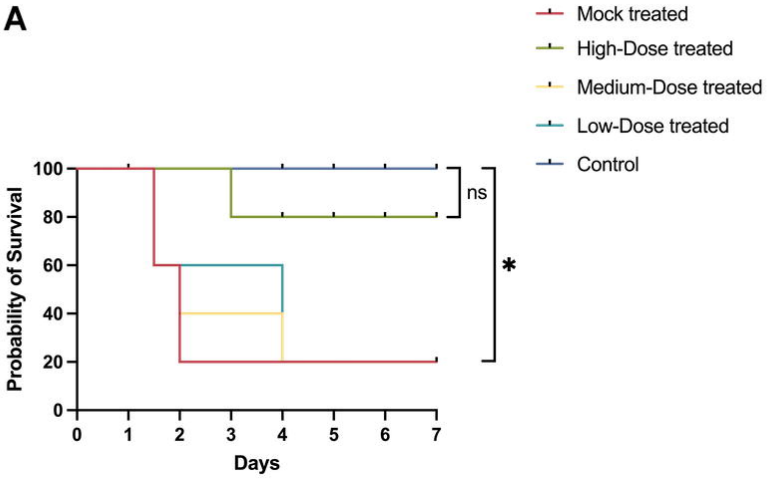
A
Mock treated
High-Dose treated
Medium-Dose treated
Low-Dose treated
Control
Probability of Survival
100
80
60
40
20
0
0
1
2
3
4
5
6
7
Days
ns
*

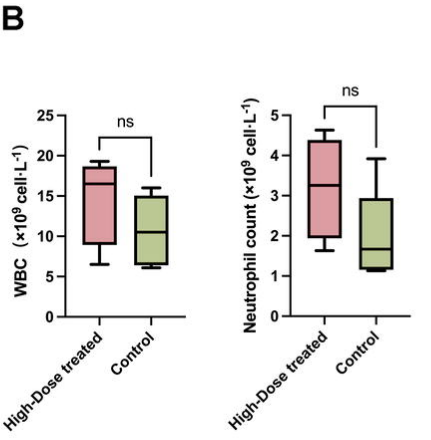
B
ns
WBC (×10⁹ cell·L⁻¹)
25
20
15
10
5
0
High-Dose treated
Control
ns
Neutrophil count (×10⁹ cell·L⁻¹)
5
4
3
2
1
0
High-Dose treated
Control

C
Control
High-dose treated
Medium-dose treated
Low-dose treated
Mock treated

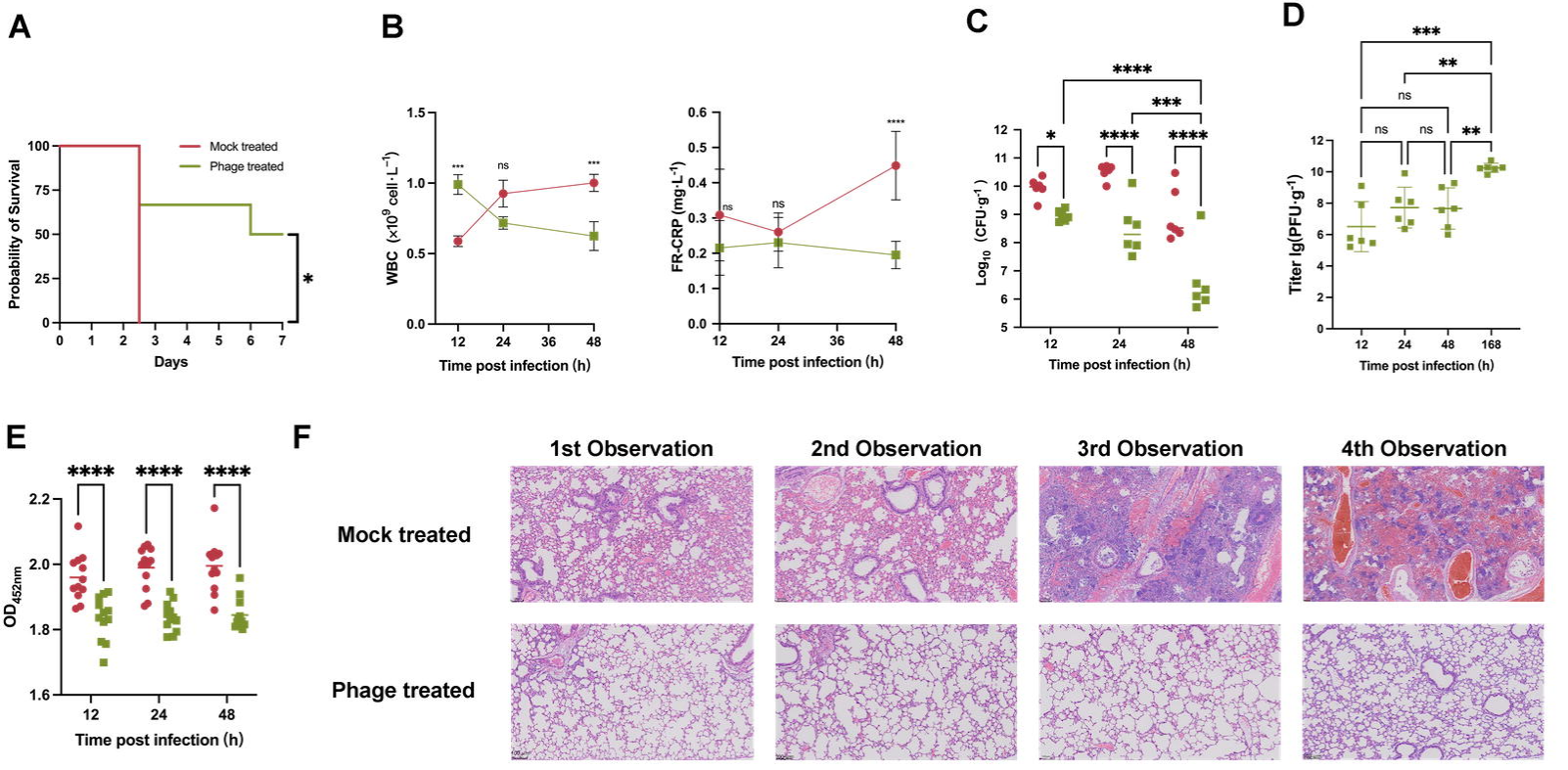
A
Mock treated
Phage treated
Probability of Survival
Days
B
WBC (×10^9 cell·L^-1)
FR-CRP (mg·L^-1)
Time post infection (h)
C
Log10 (CFU·g^-1)
Time post infection (h)
D
Titer lg(PFU·g^-1)
Time post infection (h)
E
OD452nm
Time post infection (h)
F
1st Observation
2nd Observation
3rd Observation
4th Observation
Mock treated
Phage treated